Theoretical and Applied Fracture Mechanics 145 (2026) 105627

Contents lists available at ScienceDirect

Theoretical and Applied Fracture Mechanics

journal homepage: www.elsevier.com/locate/tafmec

Finite J-integral formulation at the atomic scale and breakdown of continuum fracture mechanics

Pasquale Gallo [a,*], Takayuki Kitamura [b]

[a] Department of Industrial Engineering, University of Trento, via Sommarive 9, 38123 Trento, Italy
[b] Department of Mechanical Engineering and Science, Kyoto University, Nishikyo-ku, Kyoto 615-8540, Japan

ARTICLE INFO

Keywords:
J-integral
Atomistic fracture mechanics
Fracture process zone
Energy release rate
Brittle fracture
Nanoscale

ABSTRACT

In this work, a finite energy-based formulation of the J-integral is proposed and applied to atomic-scale defects to investigate the breakdown of continuum fracture mechanics. The J-integral is evaluated through molecular statistics simulations as the potential energy difference between two identically deformed configurations with neighbouring crack lengths, where the finite crack advance corresponds to a single atomic bond break. Single-edge cracked single-crystal silicon specimens are analyzed by progressively reducing the specimen width from the macroscale to approximately 10 nm. The results show that the critical atomistic J-integral remains essentially constant (2.5 J/m^2) across all considered sizes, demonstrating scale independence and confirming that localized bond-breaking events govern brittle fracture. The spatial extent of the fracture process zone is quantified through atomic displacement fields and is found to be approximately constant (≈0.5 nm), independent of specimen size. In contrast, the conventional continuum J-integral progressively deviates from the atomistic value when the specimen width approaches the characteristic size of the fracture process zone, indicating the breakdown of the infinitesimal crack-extension assumption. The proposed formulation provides a simple and computationally efficient framework for extending fracture mechanics concepts to the atomic scale and clarifies the physical origin of the breakdown of continuum-based fracture mechanics.

1. Introduction

Fracture mechanics has undergone significant evolution over the past decades. Central to this evolution is the concept of fracture criteria, which provides crucial insights into the initiation and propagation of cracks. Among these criteria, the J-integral, theoretically conceptualized by Eshelby in 1951, Cherepanov in 1967, and finally proposed in its modern form by Rice in 1968 [1–3], is an effective tool for characterizing crack tip fields and fracture behavior. Among its advantages: it can characterize elastic and elastic-plastic behavior; it is path-independent and, therefore, can be conveniently employed in numerical simulations; it has physical meaning given that the critical J-integral can be related to fracture toughness.

Historically, the J-integral has primarily been applied within the framework of continuum mechanics, assuming homogeneous material behavior at the macroscopic scale. However, the landscape of fracture mechanics is rapidly changing. Modern technological advancements have pushed the size of components to smaller and smaller scales, seeking high-level integration (e.g., Nano-Micro-Electromechanical Systems, nanostructured materials). In this new framework, new applications have emerged where the hypothesis of homogeneous material behavior of classical continuum mechanics is questioned. These advancements present challenges and opportunities, sparking intrigue and inspiration. Advancements in small-scale experimental techniques [4] and atomistic simulations such as molecular dynamics/statistics (MD/MS) [5,6] have supported researchers to explore fracture mechanisms at these increasingly smaller length scales, providing fascinating insights.

In particular, MD and MS simulations (as well as Density Functional Theory-DFT) have been extensively used to investigate fracture behavior at the atomic scale, primarily focusing on stress intensity factors and fracture toughness [7–13]. More recently, atomistic simulations have been extended to other well-known fracture mechanics concepts, such as energy release rate [14–17] and strain energy density [18,19]. These works show that for large samples, the conventional framework of linear elastic fracture mechanics holds well. However, when the sample's dimension is further reduced beyond the breakdown of continuum-based formulation, the strong nonlinearity that develops in a few atoms near the crack tip must be considered. In this regard, the J-

* Corresponding author.
E-mail address: pasquale.gallo@unitn.it (P. Gallo).

https://doi.org/10.1016/j.tafmec.2026.105627
Received 19 February 2026; Received in revised form 25 March 2026; Accepted 8 April 2026
Available online 9 April 2026

integral is one of the most popular concepts used for characterizing nonlinear fracture behavior.

It is intuitive that extending the J-integral to the atomic scale, where the discrete nature of atoms cannot be neglected and where continuum-based fracture mechanics breaks down due to the loss of scale separation [14,20,21], is not trivial. Early attempts based on replacing the line integral with the sum of atom-by-atom evaluation of needed parameters (e.g., traction force, strain) led to cumbersome calculation processes [22,23]. As an alternative and simpler method, equivalent domain integral approaches were proposed [24,25]. In these approaches, a weighting function considers the contribution of each atom based on spatial coordinates (examples of similar homogenization processes are also seen in non-local theories). Recently, a novel Lagrangian kernel-based estimator of continuum fields was applied to the atomic system and used to estimate the J-integral [26], showing excellent results and consistency with continuum formulation. Other researchers extended the concept of continuum J-integral to the atomistic domain by addressing challenges such as computing continuous variables from discrete atomistic quantities and incorporating nonlocality and entropic effects in atomistic computations [27]. The proposed methodology revealed many significant effects that continuum-based fracture mechanics cannot capture. A new integral scheme was recently proposed for atomically sharp cracks to push the J-integral concept beyond conventional fracture mechanics [28]. The scheme focuses on describing the local displacement gradient and stress fields when the system is discrete. Interestingly, the proposed J-integral retains path independence and still characterizes the fracture below the dimensional limit of continuum fracture mechanics.

Despite their valuable contributions, these works typically rely on complex integration schemes requiring the reconstruction of continuum-like quantities (e.g., displacement gradients or stresses) from atomistic data. Moreover, when the standard concept of the J-integral is directly transposed to atomic systems, the J-integral conceptual validity must always be verified.

The current work, instead, employs a straightforward approach to evaluate the J-integral at the atomic scale in a similar fashion to that proposed by [29] but without explicit calculation of virial stresses, displacement fields, and complex simulation schemes. By taking advantage of the energy-based definition of the J-integral, the latter is defined as a potential energy difference between two identically critically deformed samples (at the onset of crack propagation), but with neighbouring crack lengths a and $a + da$, where da is the smallest physically meaningful crack extension. Several single-edge cracked models are considered, starting from a model width W of approximately 200 nm, scaled down to approximately 10 nm. Molecular statistics (MS) analyses are then compared with continuum formulation. The validity of the continuum-based formulation is then discussed.

In contrast to existing literature, the proposed J-integral does not rely on stresses, strains, displacement fields, or contour integration, but is defined directly in terms of potential energy differences between two neighbouring crack configurations, making it naturally suited for atomistic systems. Second, the formulation requires a physically meaningful definition of the crack length increment, which is here directly linked to the discrete fracture process of single-crystal silicon, rather than treated as a numerical parameter. Third, this framework enables the identification of the regime in which classical continuum-based fracture mechanics ceases to be valid, providing a direct indication of the breakdown of the standard J-integral at small scales. Finally, it is shown that the atomically quantified J-integral is still a valid fracture criterion well beyond the limit of conventional theories.

2. Methods

2.1. Extension of the conventional J-integral

In 1968 Rice [3] presented the J-integral, a path-independent contour integral for characterizing cracks in linear and non-linear materials. By considering a counterclockwise path, Γ, around the crack tip, the integral formulation of J is given as

$$J = \int_{\Gamma} \left(w dy - T_i \frac{\partial u_i}{\partial x} ds \right) \tag{1}$$

where w, T_i, u_i and ds are the strain energy density, the component of the traction vector, the displacement vector components, and the incremental length along the path Γ, respectively. While this formulation has been extensively used at the macroscale and implemented in many commercial FEA software, evaluating the parameters atom by atom is cumbersome and challenging. On the other hand, the J-integral can also be viewed as an energy parameter [30]. Indeed, J is equal to the energy release rate in a nonlinear elastic cracked body, and relates the difference in energy absorbed by specimens with neighbouring crack sizes for elastic-plastic materials. Therefore, it can be expressed as a difference in potential energy [29,31]:

$$J = -\frac{1}{B} \frac{\partial U}{\partial a} \tag{2}$$

where U is the potential energy, B is the thickness of the sample, and a is the crack length. It must be kept in mind that the energy release rate and, in turn, the difference in potential energy must be determined by referring to the crack area, hence the introduction of thickness B in Eq. (2). For an infinitesimal crack length da, Eq. (2) can be approximated as a finite difference between two identical samples having crack length a and $a + da$ under the same critical displacement d_c of the crack length a. In the present work, d_c is defined as the displacement at the onset of crack propagation, corresponding to the first irreversible bond-breaking event at the crack tip during incremental loading. In atomistic simulations of brittle fracture, this event is followed by a rapid loss of load-carrying capacity; however, the definition adopted here is strictly based on the initiation of crack advance rather than on the subsequent global response.

In other words, the potential energy U_a of the system at the critical displacement for crack length a is first determined; then, the potential energy U_{a+da} for crack length $a + da$ is evaluated by applying d_c determined previously; finally, the J is given as the difference of these potential energies, i.e.:

$$J = -\frac{1}{B} \left(\frac{U_{a+da} - U_a}{da} \right) \tag{3}$$

The crack increment da is assumed to be small but finite (i.e., a single bond break at the crack tip as explained in the next section) and, therefore, accounts for the discrete nature of the system. This contrasts with the conventional J-integral formulation, which assumes a continuum body and infinitesimal crack advancement. Under these conditions, from a rigorous perspective, since a finite difference approximates the energy derivative, this quantity is referred to as the finite J-integral and is defined as

$$J_{AFM} = -\frac{1}{B} \left(\frac{U_{a+\Delta a} - U_a}{\Delta a} \right) = -\frac{1}{B} \left(\frac{\Delta U}{\Delta a} \right) \tag{4}$$

where AFM stands for Atomistic Fracture Mechanics, as defined by Shimada and co-workers [14,16].

Fig. 1 provides a graphical representation for the sake of clarity. With this procedure, evaluating the J-integral at the atomic scale reduces to evaluating the potential energy of two systems at the critical displacement, avoiding challenging integration schemes. Potential energy is a standard variable easily obtained from MD codes or explicitly from the potential functions.

Similarly, the critical load could be considered in substitution for the critical displacement. However, in load control, the contribution from work done by external forces is not zero and, therefore, non-negligible at

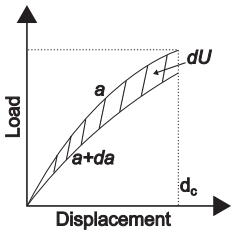

Fig. 1. Schematic representation of the potential energy difference at critical displacement d_c of two samples having neighbouring crack lengths.

such a small scale. For this reason, the critical displacement approach is simpler and straightforward.

2.2. Geometries, mechanical properties, and molecular statistics simulation

The present work has considered single-edge cracked samples made of single-crystal silicon. By referring to Fig. 2, several models have been realized, varying the width W of the sample from approximately 200 nm to 10 nm. The crack length a is kept as $W/3$ while the height is 2 W, i.e., the samples are "scaled" down. The crack is achieved by artificially removing interactions between the atoms on pre-crack surfaces.

In general, for an atomic structure, the crack extension Δa is the minimal crack extension physically possible. In the present formulation, it is therefore defined based on the discrete nature of fracture in single-crystal silicon, where crack advance occurs through successive bond-breaking events as demonstrated by several authors [10,14,18]. As a result, Δa corresponds to a single bond break at the crack tip, i.e., ≈ 0.33 nm. This is, indeed, the smallest physically meaningful increment associated with the underlying atomic structure.

The molecular statistics (MS) simulations are realized by using the well-known Large-scale Atomic/Molecular Massively Parallel Simulator (LAMMPS) molecular dynamics code [32], and the modified Stillinger-Weber (SW) interatomic potential is used [12,33,34]. SW potential is particularly suited to investigating ideal brittle fracture in silico. The orientation of the sample is depicted in Fig. 2, i.e., the crack plane coincides with the cleavage plane (111), and it is perpendicular to the direction [111]. Table 1 details the mechanical properties, lattice constant, ideal material strength (i.e., the strength of the material that is ideally defect-free), and equivalent Young's modulus E_{111} associated with the [111] direction generated by the SW potential. Several researchers have corroborated these values [16,35], which MS simulations

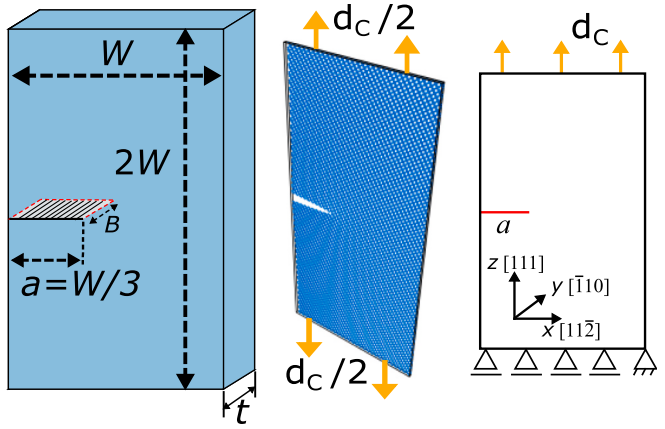

Fig. 2. Schematic representation of the sample geometry (left), the simulation box (center) at critical displacement (the crack is therefore opened for better visualization), and the FEA constraints configuration (right); W is varied from 200 nm to 10 nm approximately; t = B is constant and equal to 0.384 nm approximately.

Table 1
Lattice constant, material constants, and mechanical properties generated by the modified SW potential.

Lattice constant (Å)	C_{11}(GPa)	C_{12} (GPa)	C_{44} (GPa)	E_{111} (GPa)	σ_{IS} (GPa)
5.431	201	51.4	90.5	209	35.2

of uncracked samples can easily verify [18].

A gradual strain increase, ε, is applied to the specimens' upper and lower atomic layers, as illustrated in Fig. 2, namely mode I loading. At first, large strain increments, e.g. 0.01, are used to obtain an approximated value of the critical displacement. Subsequently, smaller strain increments, e.g. 0.0001, are employed close to the critical state to get an accurate value of the critical displacement. This approach ensures the simulations are run efficiently with a reasonable trade-off between accuracy and computational time. Periodic boundary conditions are implemented along the z-direction, equivalent to plain-strain state. The simulation box, therefore, has a finite thickness, t, in the z-direction of approximately 0.384 nm, and this is the value assumed by B in Eq. (4). At the start of the simulation and after each strain increment, relaxation is ensured using the damped dynamics method Fast Inertial Relaxation Engine (FIRE) [36] until all forces on atoms become less than $1.0 \cdot 10^{-5}$ μN.

The analysis is first done for the sample with crack length a and subsequently for the sample with finite crack advancement $a + \Delta a$. The difference in potential energy is measured when one model (crack length a) reaches a critical state (i.e., fracture) while the other model ($a + \Delta a$) maintains the same displacement under tension.

2.3. Finite element analyses (FEA)

Ansys APDL 15.0 was utilized to create sample models with a single-edge crack, as shown in the previous section. Plane strain conditions were assumed, and a 2D 8-node element-type PLANE183 was employed [37].

To ensure precision, the crack tip is represented with a "concentration key-point" [37]. A highly refined mesh was adopted in the vicinity of the crack tip, with element sizes for the smallest specimen on the order of $a/10^5$. This refined region, including the discretization used for the J-integral evaluation, was kept identical for all specimen sizes to ensure consistent resolution of the crack-tip fields. As a result, the relative refinement with respect to the crack length increases for larger specimens, leading to progressively improved resolution from the crack-tip perspective.

A mesh convergence analysis was performed for both the smallest and largest specimen sizes. The results confirm that the adopted discretization provides stable J-integral values, with no significant variation upon further refinement. Details of the mesh design and convergence study are provided in the Supplementary Material.

A linear elastic anisotropic material model was employed, and the stiffness matrix was derived from the three material constants listed in Table 1, i.e., C_{11} = 201 GPa, C_{12} = 51.4 GPa, C_{44} = 90.5 GPa. These constants correspond to an orientation identical to that used in atomistic simulations (see Fig. 2).

Fig. 2 illustrates the model's constraints configuration. The critical displacement d_c obtained from MS simulations for the sample with crack length a was applied, and the J-integral was evaluated according to the integration scheme of Eq. (1).

3. Results

Table 2 summarizes the results obtained for the considered samples. The analyses focus on W = 198.480 nm as representative of "large scale" and on W smaller than 50 nm as representative of small-scale samples. This range is defined based on conclusions from other authors showing

Table 2
Geometrical properties, boundary displacement, and external load at critical displacement for the crack length a and $a + \Delta a$; difference of potential energy and critical finite J-integral from MS simulations; the crack increment Δa is constant and equal to ≈0.33 nm (single atomic bond).

W (nm)	a (nm)	d_c (nm)	σ_a (GPa)	$\sigma_{a+\Delta a}$ (GPa)	ΔU (J)	J_{AFM} (J/m^2)
9.924	3.308	1.025	8.1773	7.8334	−3.1883E-19	2.51
19.848	6.616	1.422	5.8386	5.7184	−3.0655E-19	2.41
29.772	9.924	1.746	4.7706	4.7057	−3.0671E-19	2.41
39.696	13.232	1.999	4.1402	4.0981	−3.1507E-19	2.48
49.620	16.540	2.305	3.8348	3.8020	−3.1895E-19	2.51
101.225	33.742	3.143	2.7488	2.7001	−3.1436E-19	2.48
198.480	66.160	4.352	1.9042	1.9004	−3.1814E-19	2.50

that for W approaching 40 nm, the continuum-based formulation breaks down [14,18]. The table includes the considered geometries and the related critical quantities, i.e., boundary displacement at failure d_c, external stress at failure σ, difference of potential energy ΔU, and the finite J-integral at failure J_{AFM}, evaluated via MS simulations. For clarity's sake, J_{AFM} always refers to the atomistic J-integral, while J_{FEA} refers to the values obtained from FEA (continuum formulation).

Sample W = 9.924 nm is selected as an example to show the external load versus the boundary displacement and variation of potential energy; see Figs. 3 and 4, respectively. The same trend is found for all the samples, and redundant pictures are omitted for the sake of brevity.

It is clear from the results of J_{AFM} in Table 2 that the critical (at failure) finite J-integral is constant among different samples, regardless of the size and crack length. Even though the sample is scaled down from a crack length of 66.160 nm to 3.308 nm with a drastic reduction in the number of atoms (from 1,526,400 to 3780, respectively), the critical J_{AFM} is still, on average, 2.5 J/m^2. For a better visualization, this result is also depicted in Fig. 5. If the finite J-integral for the largest sample is taken as a reference, all the values lie within a scatter of ±5%. This result demonstrates that the J_{AFM} evaluated on atomic systems by using its potential energy formulation is constant and scale-independent when applied to single-crystal silicon, i.e., ideally brittle materials. By contrast, the J-integral values obtained from FEA and summarized in Table 3 progressively deviate from the constant trend as the specimen size decreases. It should be noted that the objective is not the direct comparison of absolute values between the two formulations, but rather

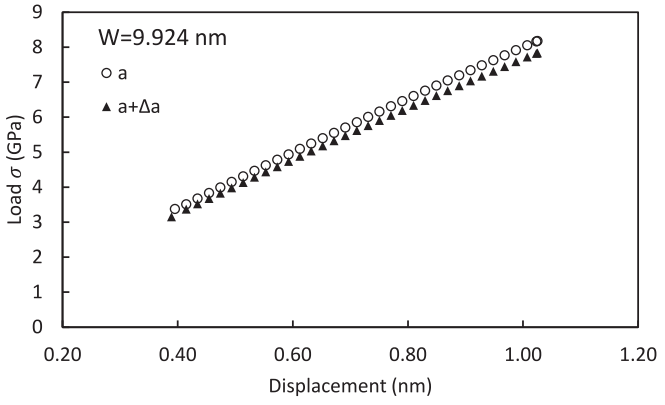

Fig. 3. Whole external (boundary) load vs. the boundary displacement for the sample W = 9.924 nm and the crack lengths a = 3.308 nm, $a + \Delta a$ = 3.638; Δa≈0.33.

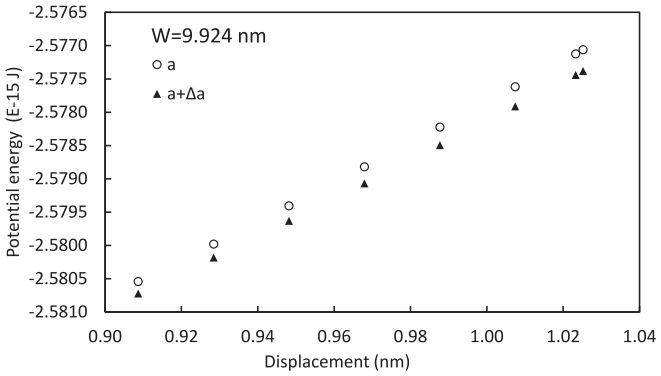

Fig. 4. Potential energy vs. the boundary displacement for the sample W = 9.924 nm and the crack lengths a = 3.308 nm, $a + \Delta a$ = 3.638; Δa≈0.33.

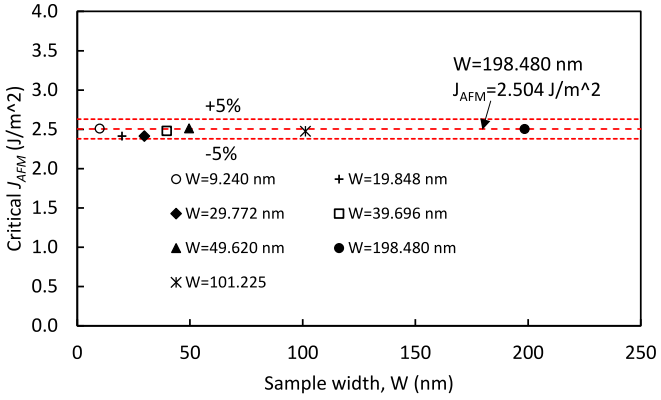

Fig. 5. Critical (at failure) J_{AFM} vs. sample width W; the dashed lines indicate the reference value for W = 198.480, and the scatter from this value (± 5%).

Table 3
J-integral values evaluated via MS simulations and FEA.

W (nm)	J_{AFM} (J/m^2)	J_{FEA} (J/m^2)
9.924	2.51	2.78
19.848	2.41	2.67
29.772	2.41	2.68
39.696	2.48	2.64
49.62	2.51	2.8
101.225	2.48	2.48
198.48	2.5	2.52

the comparison of their respective trends across scales. However, in this respect, a good agreement is observed at large specimen sizes, while systematic deviations emerge as the size decreases.

To better underline the trend and compare the results within the two formulations, Fig. 6 shows J_{AFM} and J_{FEA} normalized with respect to the J-integral obtained for the largest sample W = 198.48 nm. While the atomistic results remain essentially constant, the continuum values progressively deviate from unity as the specimen size decreases, indicating a loss of consistency of the continuum formulation at small scales. This result is further discussed in the next section.

4. Discussion

The extension of fracture mechanics concepts to length scales at which the discrete nature of matter (i.e., atoms) becomes relevant remains a central challenge in solid mechanics.

In the present work, the J-integral has been studied from an atomistic perspective by using its energy-based definition rather than its classical

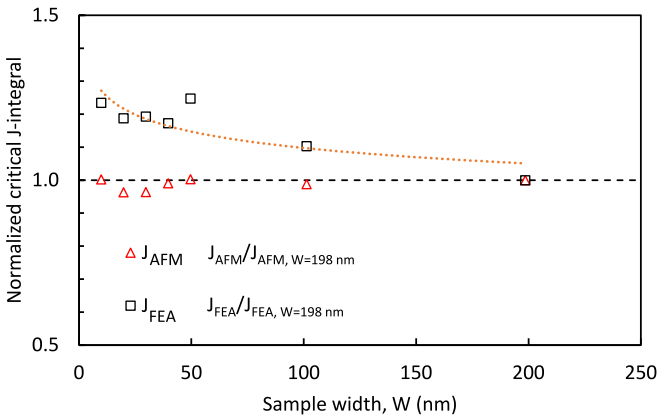

Fig. 6. Normalized critical J-integral and schematic trend for FEA results.

contour formulation. The proposed formulation is consistent with the classical energy interpretation of the J-integral as an energy release rate, since it is directly evaluated from the potential energy difference between two equilibrium configurations with neighbouring crack lengths. The results clearly show that, when evaluated as a difference in potential energy associated with an elementary but finite crack advance, the critical J-integral remains essentially constant over a wide range of specimen sizes, from the macroscale down to a few nanometers. Despite the drastic reduction in the system size and number of atoms, the critical value converges to approximately 2.5 J/m^2 as shown in Fig. 5. This result indicates that fracture is governed by atomic bond breaking and that the proposed discrete formulation captures the intrinsic fracture mechanism of ideally brittle silicon. This value is also consistent with Griffith-type energetic arguments when the appropriate crystallographic orientation is considered. In the present study, fracture occurs along the Si(111) cleavage plane. Literature surface energy, γ, values for Si(111) typically lie in the range of approximately 1.0–1.3 J/m^2, depending on reconstruction and computational methodology [12,38]. According to Griffith's condition, i.e. $G_c = 2\gamma$, this range corresponds to a critical energy release rate of approximately 2.0–2.6 J/m^2, in excellent agreement with the J_{AFM} obtained here. By contrast, higher values reported for other orientations, such as Si(110) [14], reflect the larger surface energy of that plane rather than a discrepancy in fracture formulation. When the proper cleavage plane is accounted for, the present results are quantitatively consistent with Griffith's critical energy release rate.

These observations require a careful interpretation, particularly in relation to the discrete nature of the fracture process and the role of the crack length increment Δa in the proposed formulation. In the present framework, Δa is not introduced as a numerical or tunable parameter, but is directly grounded in the discrete nature of fracture in single-crystal silicon. As demonstrated in the given references, crack advance occurs through successive bond-breaking events [14], and Δa corresponds to the smallest physically admissible increment associated with this mechanism, i.e., one atomic bond length ($\approx$ 0.33 nm). This has important consequences for the interpretation of the results. In contrast to conventional continuum or numerical formulations, where Δa may be varied to assess convergence, in the present context, it is tied to the definition of an elementary crack advance. Choosing a larger Δa would imply considering multiple bond-breaking events within a single increment, which is no longer representative of the underlying fracture mechanism and departs from the definition adopted in this work. Conversely, smaller values are not physically admissible within the atomic structure. For this reason, a standard parametric sensitivity analysis with respect to Δa is not directly meaningful in the present context.

Although $\Delta a \approx 0.33$ nm is negligible at the macroscale, it becomes comparable to characteristic dimensions as the system size decreases. As a result, the assumption of an infinitesimal crack extension, implicit in continuum fracture mechanics, no longer holds. This reflects the loss of validity of the continuum formulation as the separation of scales is reduced. In this sense, the observed discrepancy does not reflect a failure of the J concept itself, but rather a breakdown of its continuum formulation when scale separation between crack advance, fracture process zone, and stress singularity length is lost.

To further clarify the physical origin of this breakdown, it is useful to investigate the spatial extent of the atomistic fracture-dominant zone. Fig. 7 compares the atomic displacement fields in the vicinity of the crack tip for both the largest and the smallest specimens. In detail, the atomic displacement at the onset of crack propagation, Δz, was evaluated along the crack plane as a function of the distance from the crack tip, using the unloaded configuration as a reference. Considering only the upper crack-plane atoms, Δz was normalized by its maximum value at the crack-tip atom. The resulting profiles for the smallest and largest samples show that the displacement rapidly decays with increasing distance from the crack tip and becomes negligible beyond a characteristic distance. This distance defines the fracture process zone length, Λ_f. Importantly, Λ_f is found to be essentially independent of specimen width. The estimated value of Λ_f ($\approx$ 0.5 nm, see Fig. 7) is in good agreement with previously reported atomistic analyses of brittle fracture in silicon [10,14,16,18], which place the fracture-dominant zone within a few atomic spacings (on the order of 0.3–0.6 nm). This confirms that fracture at the nanoscale remains governed by a localized bond-breaking process whose spatial extent does not scale with specimen size. The fact that Λ_f is constant across scales further supports the interpretation that the critical J-integral obtained here reflects an intrinsic material property associated with atomic bond breaking, rather than a geometrical or structural size effect.

The transition from continuum to atomistic behavior can be further quantified by examining the consistency of the continuum J-integral across different specimen sizes. To this end, the J-integral values obtained from FEA are normalized with respect to the value corresponding to the largest specimen (see Fig. 6). For large specimen widths, the normalized values remain close to unity, indicating that the continuum formulation provides a consistent description of fracture. However, as the specimen width decreases below approximately 50 nm, a systematic deviation emerges and progressively increases with further size reduction.

This transition can be interpreted in relation to the ratio between the specimen width W and the characteristic fracture process zone size $\Lambda_f \approx$ 0.5 nm. When $W \gg \Lambda_f$, a clear separation of scales exists, and the continuum formulation remains valid. As W decreases and this separation is progressively lost, deviations emerge, and the continuum J-integral

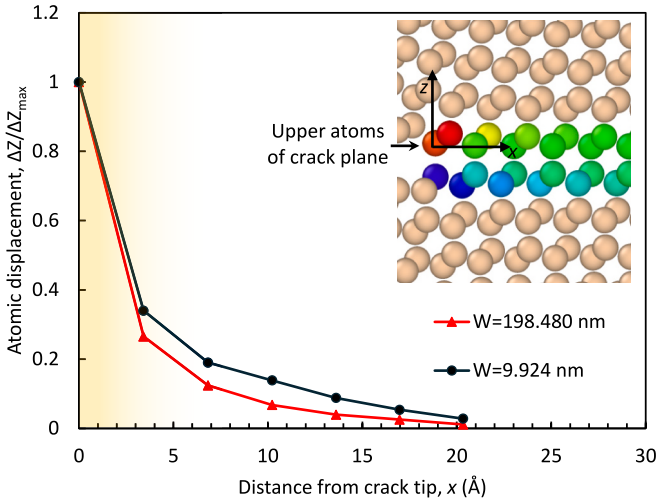

Fig. 7. Upper atoms of crack plane displacement normalized by the maximum displacement at the crack-tip, for the largest and smallest samples.

progressively loses its accuracy in describing fracture. In the present results, this transition occurs for W/Λ_f on the order of 10^2 (corresponding to $W \approx 50$ nm), and becomes increasingly pronounced as this ratio further decreases. The consistency of the FEA results with respect to mesh refinement (see Supplementary Material) confirms that the observed deviation at small scales is not a numerical artifact.

This provides a direct physical interpretation of the underlying physical assumptions of fracture mechanics. The observed deviation of the continuum J-integral should be interpreted considering the loss of scale separation between the specimen size and the fracture process zone. In the present results, the atomistic J-integral and the fracture process zone remain constant, indicating that fracture is governed by an intrinsic material length scale (i.e., atomic bond). As the specimen size approaches this characteristic length, the assumptions underlying continuum fracture mechanics are no longer satisfied. In this sense, the deviation of the continuum J-integral is not taken as evidence of breakdown per se, but as a consequence of the loss of validity of the continuum approximation.

The size range over which the continuum formulation ceases to be valid is consistent with previous studies addressing the breakdown of continuum fracture mechanics using alternative criteria such as stress intensity factor, energy release rate, and strain energy density [14,16,21,39]. These works have shown that continuum descriptions fail when the characteristic length associated with the crack-tip fields becomes comparable to the extent of the fracture process zone, i.e., when the required separation of scales is lost. Experimental evidence supporting this interpretation has also been reported, indicating that the breakdown is not an artifact of atomistic modeling but a fundamental physical limitation [40].

The present results confirm that the same physical limitation applies to the J-integral. Importantly, this conclusion is reached here through a purely energy-based formulation, without relying on the evaluation of stress fields, yet leading to a consistent identification of the transition regime. This reinforces the view that the breakdown is not specific to a particular fracture parameter, but is instead rooted in the fundamental assumptions underlying continuum mechanics.

Different fracture parameters also exhibit different sensitivities to how precisely the critical displacement is determined. Previous studies have shown that critical stress intensity factors extracted from virial stresses are often less sensitive to numerical resolution, whereas energy-based quantities such as J or G are more sensitive to discretization effects [20,41]. This behavior is consistent with the present findings and highlights the importance of carefully defining fracture criteria when transitioning from continuum to atomistic descriptions. The critical displacements obtained in the present simulations (Table 2) are in good agreement with those reported in previous works on silicon [10,18]. Minor discrepancies can be attributed to differences in strain resolution close to the onset of crack propagation. Such differences, however, cannot be used to assess which approach is more accurate. Each study is internally consistent with respect to its specific objective, whether it is the evaluation of the J-integral, the stress intensity factor, or other fracture parameters. Numerical resolution and modeling choices must therefore be evaluated in relation to the fracture quantity of interest, rather than through direct comparison of critical displacements alone.

In this context, the proposed finite J-integral formulation provides a simple and robust alternative to integration-based atomistic J-integral approaches, as it avoids the explicit reconstruction of local stress or displacement fields while retaining a clear physical meaning. Indeed, while explicit integration schemes and reconstruction of continuum-like fields at the atomic scale provide valuable insight and retain important properties such as path independence, the evaluation of local stresses and displacement could introduce an additional source of uncertainty. By contrast, the energy-difference formulation adopted here avoids these complexities and offers a straightforward and computationally efficient route to quantify fracture at the atomic scale.

Finally, some limitations of the present study should be acknowledged. The analysis is restricted to ideally brittle single-crystal silicon under mode I loading. While this allows for a clear interpretation of the fundamental mechanisms governing ideal brittle fracture at the atomic scale, extension to more complex materials and loading conditions would be useful to assess the broader applicability of the proposed approach. In particular, for materials exhibiting more ductile behavior, the definition of a physically meaningful crack length increment becomes less straightforward, as fracture involves distributed mechanisms such as plastic deformation, rather than a single bond-breaking event. Similarly, while the proposed formulation is not inherently restricted to mode I loading, its extension to mixed-mode conditions requires verification of the underlying fracture mechanisms and the associated crack advance at the atomic scale. Moreover, the MS analyses are conducted under 0 K conditions, enabling a clear identification of the energy associated with elementary crack advance; the influence of thermal fluctuations is not considered here and is left for future investigation.

Nevertheless, the results demonstrate that the proposed finite, energy-based J-integral formulation provides a consistent and physically meaningful fracture criterion well beyond the limits of conventional continuum theories.

5. Conclusions

This work investigated the applicability of the J-integral as a fracture criterion at the atomic scale through a finite, energy-based formulation within molecular statistics simulations of single-crystal silicon. By defining the J-integral as the potential energy difference between two critically deformed configurations with neighbouring crack lengths, fracture behavior was consistently characterized from the macroscale down to nanometric dimensions.

The main conclusions are:

- The atomistic finite J-integral J_{AFM} remains essentially constant (2.5 J/m^2) over a wide range of specimen sizes, demonstrating scale independence and confirming that brittle fracture in silicon is governed by atomic bond breaking.
- The crack length increment Δa is defined as the smallest physically admissible crack advance (single bond-breaking event of ≈0.33 nm for single-crystal silicon), ensuring that the formulation is grounded in the underlying fracture mechanism rather than in a numerical parameter choice.
- The spatial extent of the fracture process zone, quantified through atomic displacement fields, is approximately constant ($\Lambda_f \approx 0.5$ nm) and independent of specimen width. This confirms that fracture is controlled by a localized bond-breaking mechanism whose characteristic size does not scale with geometry.
- The loss of scale separation between significant quantities (e.g. fracture process zone, specimen width) rather than the failure of a specific fracture parameter, is the fundamental reason for the deviation of continuum predictions at the nanoscale.
- The conventional continuum formulation of the J-integral progressively deviates from the atomistic results as the specimen size decreases and ultimately fails to characterize fracture at the nanoscale.
- The proposed finite difference formulation provides a simple, physically transparent, and computationally efficient alternative to integration-based atomistic J-integral approaches, preserving a direct link between fracture energy and atomic bond breaking.

CRediT authorship contribution statement

Pasquale Gallo: Writing – review & editing, Writing – original draft, Visualization, Methodology, Investigation, Formal analysis, Conceptualization. **Takayuki Kitamura:** Writing – review & editing, Conceptualization.

Funding

This research did not receive any specific grant from funding agencies in the public, commercial, or not-for-profit sectors.

Declaration of competing interest

The authors declare that they have no known competing financial interests or personal relationships that could have appeared to influence the work reported in this paper.

Appendix A. Supplementary data

Supplementary data to this article can be found online at https://doi.org/10.1016/j.tafmec.2026.105627.

Data availability

Data will be made available on request.

References

[1] G.P. Cherepanov, Crack propagation in continuous media, J. Appl. Math. Mech. 31 (1967) 503–512, https://doi.org/10.1016/0021-8928(67)90034-2.
[2] J.D. Eshelby, The force on an elastic singularity. Philosophical Transactions of the Royal Society of London Series A, Mathematical Phys. Sci. 244 (1951) 87–112, https://doi.org/10.1098/rsta.1951.0016.
[3] J. Rice, A path independent integral and the approximate analysis of strain concentration by notches and cracks, J. Appl. Mech. 35 (1968) 379–386.
[4] J. Ast, M. Ghidelli, K. Durst, M. Göken, M. Sebastiani, A.M. Korsunsky, A review of experimental approaches to fracture toughness evaluation at the micro-scale, Mater. Des. 173 (2019) 107762, https://doi.org/10.1016/j.matdes.2019.107762.
[5] T. Shimada, T. Kitamura, Fracture mechanics at atomic scales, in: H. Altenbach, T. Matsuda, D. Okumura (Eds.), Advanced Structured Materials 64, Springer International Publishing, Cham, 2015, pp. 379–396, https://doi.org/10.1007/978-3-319-19440-0_17.
[6] S.P. Patil, Y. Heider, A review on brittle fracture nanomechanics by all-atom simulations, Nanomaterials 9 (2019) 1–31, https://doi.org/10.3390/nano9071050.
[7] N. Yanagida, O. Watanabe, Molecular dynamics simulation of effects of lattice orientation on crack propagation in alpha-Iron when the primary slip direction is in the plane of tensile stress, JSME Int. J. Ser A, Mech. Material Eng. 39 (1996) 321–329, https://doi.org/10.1299/jsmea1993.39.3_321.
[8] O. Kamigaito, Ideal fracture stress of brittle material having no defect, J. Mater. Sci. Lett. 7 (1988) 529–531, https://doi.org/10.1007/BF01730717.
[9] M.Q. Le, R.C. Batra, Mode-I stress intensity factor in single layer graphene sheets, Comput. Mater. Sci. 118 (2016) 251–258, https://doi.org/10.1016/j.commatsci.2016.03.027.
[10] P. Gallo, On the crack-tip region stress field in molecular systems: the case of ideal brittle fracture, Adv. Theory Simul. 2 (2019) 1900146, https://doi.org/10.1002/adts.201900146.
[11] G.H. Lee, Y.J. Chung, S.M. Na, H.G. Beom, Atomistic investigation of the t-stress effect on fracture toughness of copper and aluminum single crystals, J. Mech. Sci. Technol. 32 (2018) 3765–3774, https://doi.org/10.1007/s12206-018-0729-0.
[12] D. Holland, M. Marder, Ideal brittle fracture of silicon studied with molecular dynamics, Phys. Rev. Lett. 80 (1998) 746–749, https://doi.org/10.1103/PhysRevLett.80.746.
[13] P. Andric, W.A. Curtin, Atomistic modeling of fracture, Model Simul. Mat. Sci. Eng. 27 (2019) 013001, https://doi.org/10.1088/1361-651X/aae40c.
[14] T. Shimada, K. Ouchi, Y. Chihara, T. Kitamura, Breakdown of continuum fracture mechanics at the nanoscale, Sci. Rep. 5 (2015) 8596, https://doi.org/10.1038/srep08596.
[15] T. Sumigawa, T. Shimada, S. Tanaka, H. Unno, N. Ozaki, S. Ashida, et al., Griffith criterion for nanoscale stress singularity in brittle silicon, ACS Nano 11 (2017) 6271–6276, https://doi.org/10.1021/acsnano.7b02493.
[16] K. Huang, T. Shimada, N. Ozaki, Y. Hagiwara, T. Sumigawa, L. Guo, et al., A unified and universal Griffith-based criterion for brittle fracture, Int. J. Solids Struct 128 (2017) 67–72, https://doi.org/10.1016/j.ijsolstr.2017.08.018.
[17] P. Jia, K. Huang, T. Sumigawa, T. Shimada, L. Guo, T. Kitamura, A unified atomic energy release rate criterion for nonlinear brittle fracture in graphene nanoribbons, Int. J. Solids Struct. (2021) 111260, https://doi.org/10.1016/j.ijsolstr.2021.111260.
[18] P. Gallo, Y. Hagiwara, T. Shimada, T. Kitamura, Strain energy density approach for brittle fracture from nano to macroscale and breakdown of continuum theory, Theoretical Appl. Fracture Mech. 103 (2019) 102300, https://doi.org/10.1016/j.tafmec.2019.102300.
[19] P. Gallo, T. Sumigawa, T. Kitamura, F. Berto, Static assessment of nanoscale notched silicon beams using the averaged strain energy density method, Theor. Appl. Fract. Mech. 95 (2018) 261–269, https://doi.org/10.1016/j.tafmec.2018.03.007.
[20] T. Shimada, K. Huang, L. Van Lich, N. Ozaki, B. Jang, T. Kitamura, Beyond conventional nonlinear fracture mechanics in graphene nanoribbons, Nanoscale 12 (2020) 18363–18370, https://doi.org/10.1039/d0nr03836a.
[21] P. Gallo, T. Sumigawa, T. Shimada, Y. Yan, T. Kitamura, Investigation into the breakdown of continuum fracture mechanics at the nanoscale: Synthesis of recent results on silicon, in: E.E. Gdoutos (Ed.), Proceedings of the First International Conference on Theoretical, Applied and Experimental Mechanics, Springer International Publishing, Cham, 2019, pp. 205–210, https://doi.org/10.1007/978-3-319-91989-8_45.
[22] R. Miller, E.B. Tadmor, R. Phillips, M. Ortiz, Quasicontinuum simulation of fracture at the atomic scale, Model Simul Mat Sci Eng 6 (1998) 607–638, https://doi.org/10.1088/0965-0393/6/5/008.
[23] H. Inoue, Y. Akahoshi, S. Harada, A fracture parameter for molecular dynamics method, Int J Fract 66 (1994) R77–R81, https://doi.org/10.1007/BF00018446.
[24] K. Nakatani, A. Nakatani, H. Kitagawa, Molecular Dynamics Study on Fracture Mechanism of Fe-Amorphous Metal (J Integral near Mode I Crack Tip), 1998, pp. 88–98, https://doi.org/10.1007/978-3-662-35369-1_7.
[25] Y. Jin, F.G. Yuan, Nanoscopic modeling of fracture of 2D graphene systems, J. Nanosci. Nanotechnol. 5 (2005) 601–608, https://doi.org/10.1166/jnn.2005.071.
[26] R.E. Jones, J.A. Zimmerman, The construction and application of an atomistic j-integral via hardy estimates of continuum fields, J. Mech. Phys. Solids 58 (2010) 1318–1337, https://doi.org/10.1016/j.jmps.2010.06.001.
[27] S. Roy, A. Roy, A computational investigation of length-scale effects in the fracture behaviour of a graphene sheet using the atomistic j-integral, Eng. Fract. Mech. 207 (2019) 165–180, https://doi.org/10.1016/j.engfracmech.2018.12.012.
[28] P. Jia, K. Huang, H. Yu, T. Shimada, L. Guo, T. Kitamura, A novel atomic j-integral concept beyond conventional fracture mechanics, Theor. Appl. Fract. Mech. 121 (2022), https://doi.org/10.1016/j.tafmec.2022.103531.
[29] Y.G. Xu, K. Behdinan, Z. Fawaz, Molecular dynamics calculation of the j-integral fracture criterion for nano-sized crystals, Int J Fract 130 (2004) 571–583, https://doi.org/10.1023/B:FRAC.0000049499.53799.b7.
[30] T.L. Anderson, Fracture Mechanics: Fundamentals and Applications, Third Edition, Taylor & Francis, 2005.
[31] J.A. Begley, J.D. Landes, The J integral as a fracture criterion.pdf, 1972.
[32] S. Plimpton, Fast parallel algorithms for short-range molecular dynamics, J. Comput. Phys. 117 (1995) 1–19, https://doi.org/10.1006/jcph.1995.1039.
[33] D. Holland, M. Marder, Cracks and atoms, Adv. Mater. 11 (1999) 793–806, https://doi.org/10.1002/(SICI)1521-4095(199907)11:10<793::AID-ADMA793>3.0.CO;2-B.
[34] F.H. Stillinger, T.A. Weber, Computer simulation of local order in condensed phases of silicon, Phys. Rev. B 31 (1985) 5262–5271, https://doi.org/10.1103/PhysRevB.31.5262.
[35] J.J. Wortman, R.A. Evans, Young's modulus, shear modulus, and poisson's ratio in silicon and germanium, J. Appl. Phys. 36 (1965) 153–156, https://doi.org/10.1063/1.1713863.
[36] E. Bitzek, P. Koskinen, F. Gähler, M. Moseler, P. Gumbsch, Structural relaxation made simple, Phys. Rev. Lett. 97 (2006) 170201, https://doi.org/10.1103/PhysRevLett.97.170201.
[37] E. Mandenci, I. Guven, The Finite Element Method and Applications in Engineering Using ANSYS, Springer, 2006.
[38] R. Pérez, P. Gumbsch, An ab initio study of the cleavage anisotropy in silicon, Acta Mater. 48 (2000) 4517–4530, https://doi.org/10.1016/S1359-6454(00)00238-X.
[39] F. Liu, Q. Tang, T.C. Wang, Intrinsic notch effect leads to breakdown of Griffith criterion in graphene, Small 1700028 (2017) 1–8, https://doi.org/10.1002/smll.201700028.
[40] K. Huang, T. Sumigawa, T. Shimada, S. Tanaka, Y. Hagiwara, L. Guo, et al., An experimental study on atomic-level unified criterion for brittle fracture, Int. J. Solids Struct. 206 (2020) 1–8, https://doi.org/10.1016/j.ijsolstr.2020.08.006.
[41] T. Kitamura, T. Sumigawa, H. Hirakata, T. Shimada, Fracture Nanomechanics, 2nd ed, Pan Stanford Publishing, Singapore, 2016.